# Quantifying Effects of Cutting and Welding on Magnetic Properties of Electrical Steels

Konstantinos Bourchas, Alexander Stening, Juliette Soulard, Arvid Broddefalk, Magnus Lindenmo,
Mats Dahlén, and Freddy Gyllensten

*Abstract* — The magnetic properties, namely the iron losses and the relative permeability, of SiFe electrical steel laminations after guillotine shearing and cutting by means of fiber and CO2 lasers are studied. The magnetic measurements are conducted on the Epstein frame for lamination strips with 1, 2, and 3 additional cutting edges along their length, in order to increase the cutting effect and the characterization data. The quantified effects of manufacturing (cutting and welding) are presented for three different material grades: M270-50A, M400-50A, and a non)oriented electrical steel of gauge 0.2 mm called NO20. Usage of the Epstein frame method allows any electrical steel company to reproduce the measurements for any specific grade. Data presented in normalized values facilitate utilization of the presented results and comparison between materials. An original model that incorporates the cutting effect considering homogenously damaged areas is developed and implemented in a finite-element method-based motor design software. Its originality is that it includes dependence on the geometry, included in the material magnetic properties. Simulations made for an industrial low voltage induction motor indicate a more than 15% increase in the iron losses compared with a model that does not consider the mechanical cutting effect. In the case of laser cutting, this increase reaches 30% to 50%, depending on laser settings. These relatively large increases of iron losses justify the implementation of the effect of cutting in industrial finite-element design tools, using a method that does not increase the simulation time.

Index Terms—Cutting effect, electrical steel, finite-element method (FEM), fiber laser, guillotine, iron losses, laser settings, relative permeability, welding.

## I. Introduction

The electrical steel laminations used in the stator and rotor cores of electrical machines are typically obtained by cutting through punching or laser. Punching is normally used in mass production while laser cutting is mainly used for prototype motors or small-scale production, since punching tools investments normally imply relatively high costs. The manufacturing process damages the magnetic properties of electrical steel laminations used in electrical machines. The deterioration needs to be quantified so that machine performance can be predicted accurately from design stage. Design tools usually involve analytical models complemented with the finite-element method (FEM) simulations. The aim of this study is to introduce the quantified effects of manufacturing in these tools with as less as possible changes in the implemented models. The originality of the approach is that it is strongly influenced by the industrial context the authors are active within, compared to most methods and investigations described in the literature that are developed within the research environment with different time, cost, and human resources constraints.

Key material parameters such as B(H) curves and iron loss coefficients for calculation models are investigated. Such data are usually obtained from certificates or datasheets made available by electrical steel manufacturers using Epstein frame measurements [1], or in some cases from other methods [2]. The capability of any electrical steel manufacturer to reproduce the presented experiments since they have in-house Epstein frame measurements capabilities is a fundamental feature at the core of this paper.

Section II is dedicated to a review of the selective literature in the area to justify the scope of the investigations presented in Section III. The studies of cutting effects for both guillotine shearing (assumed equivalent to punching) and laser cutting, with a wide range of settings, are investigated. With different thicknesses and widths of lamination samples, geometrically related dependences of the magnetic properties are derived in Section IV. The effect of welding is described in Section V. This extensive measurement campaign enables adequate material data to be utilized in 2-D FEM simulations of motor performances in Section VI. Section VII is dedicated to discussing the advantages and limitations of the presented investigations and method, especially with regard to literature not considered during the project time. Conclusions are drawn in Section VIII.

## II. LITERATURE REVIEW

Mechanical cutting induces large mechanical deformations  and residual stresses in electrical steels, leading to deterioration of the magnetic properties. In [3], combined Epstein and hardness measurements on 1% Si steel laminations indicated a stressed region up to 0.35 mm. In [4], magnetic measurements on ring core topology are designed based on the assumption that the stressed region may expand up to 10–20 mm from the cutting edge. In [5], measurements with single-sheet tester (SST) showed that mechanical cutting causes a power loss increase up to 30% as well as a significant change in the B(H) curves of the magnetic material. This was measured at 0.9 T, 50 and 400 Hz, strip width of 12.5 mm, with a material called M400-50AP (3.7 W/kg at 1.5 T and 50 Hz). Similar measurements in [6] show that the magnetic degradation of non-oriented electrical steels is lower for sheets with reduced thickness. In the same reference, it is also found that cutting has a larger impact on the magnetic properties of electrical steels with high Si content.

Laser cutting causes thermal residual stresses at the edges of the electrical steel laminations [7]. In [8], Epstein measurements on 2% SiFe steel indicate 6% higher losses for laser cut laminations compared with punched ones at 1.5 T, 60 Hz. In [9], two settings of CO2 laser with different power and speed are studied. It is found that laser cutting on 0.3% and 3% Si laminations is more appropriate than mechanical cutting when the samples are 5 mm wide, while X-ray analysis reveals that laser causes higher residual stresses than mechanical cutting. In [10], eight settings with varying power, speed, and assisting gas pressure are tested on CO2 laser as well. Three different materials of 0.65 mm thickness were characterized, all with less than 1% Si content. Interestingly, both the chemical composition and the grain size of the different grades are reported. SST measurements reveal that the losses after laser cutting are up to 15% higher than the corresponding losses after mechanical cutting. In the case of laser cut samples, higher field strength is required to reach a certain level of induction. More studies using SST are given in [11] and [12]. In [11], only CO2 laser was investigated with 120 × 120 mm sheet samples, and 4-mm wide samples showed a doubling of the iron losses compared to full-size sample at 1 T, 50 Hz. The study in [12] used spark erosion as reference as well as sheet samples 150 × 150 mm. At 1 T, 50 Hz, the iron losses are 60% higher for guillotine and 6-mm-wide samples compared to spark erosion for 150-mm wide samples. The corresponding number is 125% for laser cut120ting under the same condition, leading to an increase of around 40% more losses from laser to guillotine cutting for really thin samples. In [13], Epstein and stator stack measurements conducted on SiFe laminations indicate that solid-state laser cutting and CO2 laser cutting cause similar increase in the specific losses. In [14], the lowest iron losses are seen in test samples manufactured using fast laser cutting. Furthermore, cutting is found to affect hysteresis losses more than eddy-current losses [15]–[17].

An alternative test approach using a needle probe instrument is described in [18], where it is shown that larger punching clearance causes larger negative effect on magnetic performance, and that materials with smaller grain size have less deformations and resulting magnetic deterioration.

The idea of using a degradation zone from the cut edge of an electrical steel sample for improving loss modeling and calculation tools is presented in [12], [14], [15], and [19]–[22]. The analysis of the measurements differs based on the usage of the extracted data in the design tools. Three approaches may be separated among the selected set of references. The first approach is to determine equivalent material characteristics assuming the sample width is uniformly damaged (easy to implement in FEM models but not physically accurate) [12], [14], [15], [19]. The second approach is based on identification of the width of the damaged area and its material properties, defining thin regions along the cut edges in the FEM geometry with different magnetic properties [20], [21]. The third and most recently proposed approach is to define a “continuous damaged area” where the magnetic properties evolve with the distance to the cut edge in a discretized way following the mesh pattern. This requires the use of a specially developed FEM package where the magnetic properties of each mesh element can be specified [22].

In welding processes, the lamination stack of the core is assembled through welding seams in the direction of the active length of the machine. During such processes, mechanical and thermal residual stresses are induced and degrade the magnetic properties of the material [23]. Additionally, welding causes short circuits between the laminations which decrease the effective resistivity of the core and therefore increases eddy current losses [24]. In [23], magnetic measurements on a ring core topology are performed and the results indicate that as the number of welding seams increases there is an increase in the iron losses and a drop in the permeability. In [25], the welding effect is investigated on a ring core topology with eight welding seams and NO20 laminations. The results are compared to a non-welded, taped core and the outcome is that the magnetic properties of the material are significantly degraded and the total specific iron losses increased. In [16], the authors investigate the welding effect on a stator core topology. As reference, a taped stator core is used and the studied core has 12 welding seams. It is shown that the increase in losses due to welding is less significant at higher frequencies and induction levels.

The references in the literature review described above give guidelines that are really useful in order to understand possible degradation of magnetic properties caused by manufacturing effects. However, the applicability of published results in electrical machine modeling is not straightforward for arbitrary machine designs and electrical steel grades. It was shown in [18] that two materials performing similarly at 50 Hz (i.e., would be given the same grade labeling) can actually have different chemical compositions and a major variation in grain size. The investigated material with small grain was far less sensitive to manufacturing effects than the one with large grain. The grain size influences the mechanical properties of the material and thus the details of the deformation behavior during the cutting operation. This knowledge practically means that previously published experimental data for a given grade to quantify manufacturing effects at device level can only be used in a meaningful way, if detailed information about material (i.e., chemical composition and mechanical properties) is also provided together with the material grade.

## III. SCOPE OF THE INVESTIGATIONS

With the aim to introduce the quantified effects of manufacturing in traditional design tools, with as less as possible changes in the implemented FEM models, it was chosen to use the standard test method for magnetic material characterization, namely measurements with the 25 cm Epstein frame, which follows the IEC 404-2 standard [1]. This is also the normal method used by electrical steel manufacturers for presenting magnetic properties of different lamination grades, which is commonly used as input data for FEM simulations in electrical machine analysis. Considering these tests values as reference makes the comparisons fully transparent. Consequently, in the next sections, the measurement results on strips with different widths are presented in per unit form, with the results for the standard strip width of 30 mm as the references, so that the relative degradation is visible directly. There is no need to identify a degradation depth with the presented method.

The proposed model is particularly adapted to describe what happens in the teeth of electrical machines, since the flux direction for each individual tooth is mainly 1-D (radial) as in the Epstein test strips. It is assumed to be appropriate for simplistically representing the yoke characteristics, since the larger regions with the highest flux densities in normal duty also involve flux that is relatively uniform (tangential).

Three types of non-oriented electrical steel laminations are tested [26], [27]. The specimens are selected so that two laminations with the same Si content and different thickness, as well as two laminations with different Si content and the same thickness are included. The first one is a lamination with 1.8% Si content and 0.5 mm thickness (M400-50A). The other two types of laminations have 3.2% Si content, while their thickness is 0.5 and 0.2 mm (M270-50A and NO20, respectively).

Instead of punching, guillotine shearing is performed in this study. In [16], the effects of guillotine shearing and punching with a new and a worn tool were compared. The iron losses increased by maximum 4% with the worn punching tool compared to guillotine shearing for M270-50A, but were 1% lower with the new punching tool for M400-50A. Therefore, it is assumed in this study, for practical reasons, that the effects of punching and guillotine shearing are equal. For laser cutting, both fiber and $CO_2$ lasers are used. The influence of welding is investigated by comparing non-welded specimens with welded specimens of various numbers of welding seams.

The measurements concern in this case sinusoidal magnetic polarizations up to 1.7 T at frequencies of 50, 100, and 200 Hz.


Fig. 1. (a) Photographs of the Epstein frame used in measurements.
(b) Zoom of the bottom right corner of the Epstein frame showing 10-mm-wide test samples.

# IV. CUTTING EFFECT

## A. Guillotine Shearing

According to IEC 404-2, which is the standard regarding the Epstein measurements [1], the width of the strips under test should be 30 mm. In order to increase the cutting effect, the studied samples are cut along their length in 1/2, 1/3, and 1/4 widths, and assembled in parallel during tests, in order to maintain the standard 30 mm total width. The study therefore includes strip widths of 30, 15, 10, and 7.5 mm, which enables comprehensive data. Fig. 1 shows the Epstein frame loaded with the set of 10-mm-wide samples (zoom of the corner). Figs. 2 and 3 illustrate the increase of the total specific loss and the reduction of the relative permeability as a function of the polarization.

The specimen is based on M270-50A and the reference is the standard Epstein strip (30 mm wide). The relative increase of the total specific loss gets lower with increased induction. The largest deviation in relative permeability between a 30 mm and a 7.5 mm wide strip is 61% at 1.3 T, corresponding to the “knee” in the $B(H)$ curve. Cutting also modifies the hysteresis loop of the material, as can be seen in Fig. 4, where the effect on M270-50A for a standard Epstein strip (30 mm) and a 7.5 mm wide strip is illustrated. The maximum applied field strength was selected to create a peak polarization of 1.5 T. The coercive field increases, while the remanence decreases for the narrower strip width case. One reason for the drop of remanence is the residual stresses in the material which causes magnetic anisotropy [7]. The increase of coercive field strength indicates an increase of the hysteresis losses due to plastic deformation caused by shearing, or thermal residual stresses in the case of laser cutting (as seen in Fig. 11).The induced microscopic residual stresses hinder the motion of the domain walls, also called pinning [7].

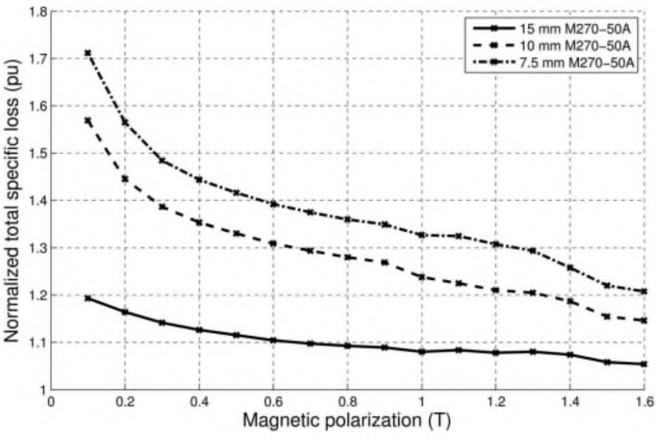


Fig. 2. Normalized total specific loss of M270-50A at 50 Hz mechanically cut in different widths, with the standard Epstein strip (30 mm wide) as reference.

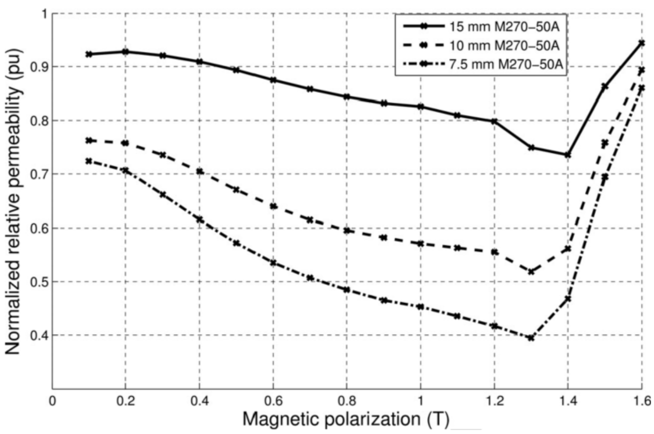


Fig. 3 Normalized relative permeability of M270-50A at 50 Hz mechanically cut in different widths, with the standard Epstein strip as reference

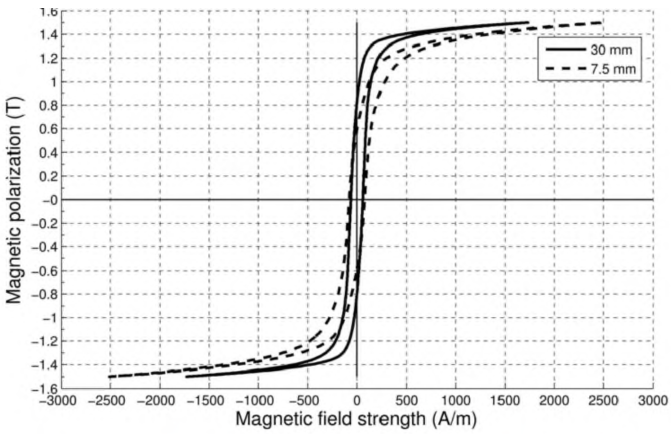


Fig. 4. Hysteresis loops of mechanically cut M270-50A at 50 Hz for two different strip widths.

Figs. 5 and 6 illustrates the degradation trend as a function of mechanically cut strip width of the total specific loss and the relative permeability, respectively, of the three tested laminated materials for three different magnetic polarizations of 0.5, 1, and 1.5 T at the frequency 50 Hz. Figs. 7 and 8 extend the statistical data further by including the frequency dependence for a strip width of 7.5 mm.

The curve in Fig. 5 for M400-50A at 1 T and 50 Hz for 10-mm and 15-mm-wide samples can be compared to results presented in [28]. The values are the same within measurement and curve reading accuracy. Since this reference tested the same grade as in this paper, from the same manufacturer using the same method with Epstein frame measurements, it gives credibility that the material data can be reproduced. It also shows that the different batches from the same manufacturer do not show drastic variation between 2008 and 2015. NO20 shows the lowest degradation, which means that a thinner lamination thickness results in a lower material degradation. Similar results are found in [6]. Among the laminations with the same thickness, the one with higher Si content (M270-50A) shows higher degradation at low induction, but at higher induction than 0.6 T the relative difference is small, as seen in Fig. 7. This result is in line with what is found in [6] and [9]. The frequency is found to have a relatively minor degradation effect on the normalized total specific loss and normalized relative permeability. The degradation is higher at decreasing induction levels, for instance illustrated by the steel grade M270-50A, which has around 20% higher relative loss at 1.5 T and as much as 50–70% higher at 0.1 T, as seen in Fig. 7.

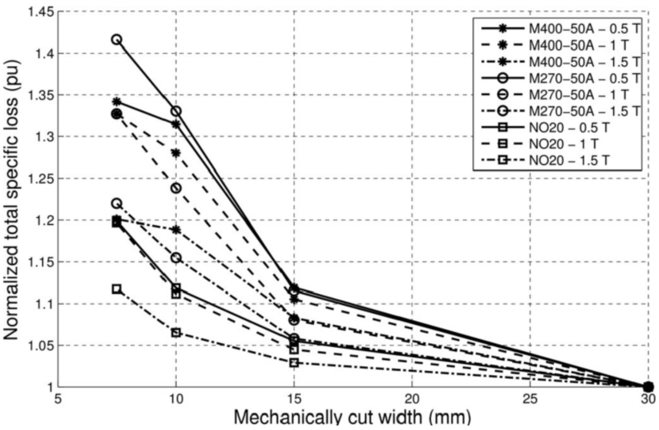


Fig. 5. Normalized total specific loss as a function of the strip width, at 50 Hz and at three different polarizations of 0.5, 1, and 1.5 T, with the standard Epstein strip (30mm) as reference

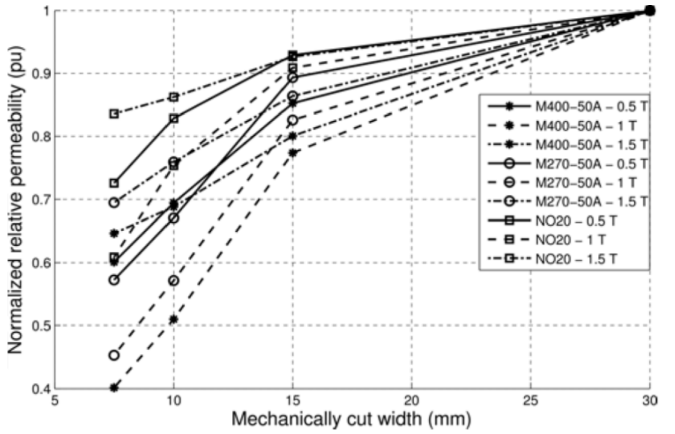


Fig. 6 Normalized relative permeability as a function of the strip width, at 50 Hz and at three different polarizations of 0.5, 1, and 1.5 T, mechanically cut with the standard Epstein strip (30 mm wide) as reference.

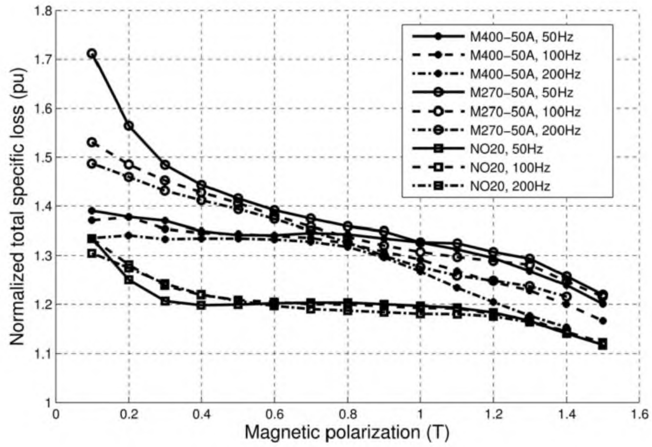


Fig. 7. Normalized total specific loss as a function of magnetic polarization, at different frequencies for a strip width of 7.5 mm, mechanically cut with the standard Epstein strip (30 mm wide) as reference.

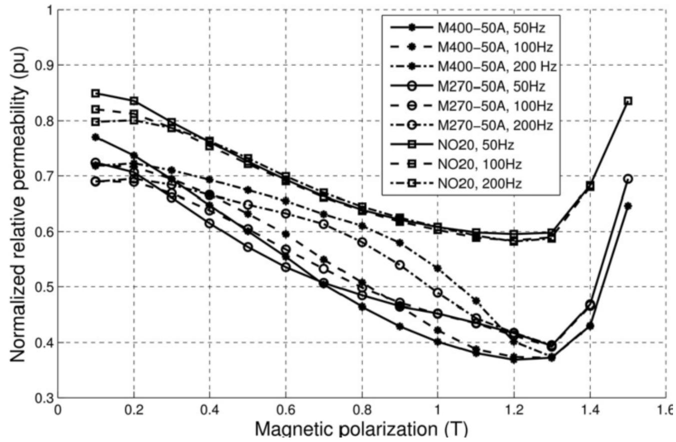


Fig. 8. Normalized relative permeability as a function of magnetic polarization, at different frequencies for a strip width of 7.5 mm, mechanically cut with the standard Epstein strip (30mm) as reference

The measurement results indicate that grade materials with thinner steel thicknesses have lower magnetic degradation, i.e., the deviation from original performance data is smaller, when mechanically cut in thinner strip widths than 30 mm. This is only based on observations of the results. NO20 and M270-50A are two steel grades that come from the same raw material. The main difference is in the lamination thickness 0.2 and 0.5 mm, respectively. The nominal chemical composition of the grades in this specific case is the same and the typical mechanical properties are very similar.

## B. Laser Cutting

In this study, cuttings with both fiber and $CO_2$ lasers are performed. Particularly, different settings of the fiber laser and one default setting of the $CO_2$ laser are tested. Each setting consists of four variables: 1) power; 2) cutting speed; 3) frequency; and 4) pressure of the assisting gas. The settings are tuned empirically in order to improve the cutting results. Figs. 9 and 10 illustrate the degradations on losses and relative permeability of M400-50A, for a strip width of 10 mm, after cutting with the settings that result in the best and the worst magnetic properties. The laser setting with the highest power and the highest speed, out of the tested settings, results in the best magnetic characteristics, which is in line with results in [14]. Due to the high speed, the productivity of the cutting tool can increase while keeping the magnetic degradation in the lowest possible level (lowest among the tested settings). On the other hand, the setting with the highest power and the lowest speed introduces the maximum degradation, and is therefore the worst. The settings for frequency and gas pressure are equal for the laminations that result into the best and the worst samples. Fiber laser is also found superior to $CO_2$ laser regarding the magnetic properties of the cut material. Fiber laser has smaller wavelength than CO2 laser, with around 1 µm versus 10 µm, which can produce an extremely small spot size, around 100 times smaller area than for CO2 laser.

When comparing the normalized total specific loss given in Fig. 9 for mechanically cut and best laser cut strips, respectively, it is seen that both methods have the same loss increase of around 20% at 1.5 T, while the laser cut strips have higher losses for lower induction levels. Analogously, when comparing the relative permeability in Fig. 10, a similar trend in relative performance is seen. However, above 1.3 T, the degradation is lower for the best laser cut steel, indicating that the saturation level is higher than for mechanical cut steel. This fact is also supported by the hysteresis loop in Fig. 11, where it can be seen that the magnetic field strength is lower for laser at an induction of 1.5 T, when comparing with the hysteresis loop from mechanically cut samples in Fig. 4. The hysteresis loop of the laser cut material is more deformed compared to the mechanically cut one, as shown in Fig. 11, for strip widths of 30 and 7.5 mm. This deformation can be seen around the origin of the axis, i.e., for low values of polarization and magnetic field strength.

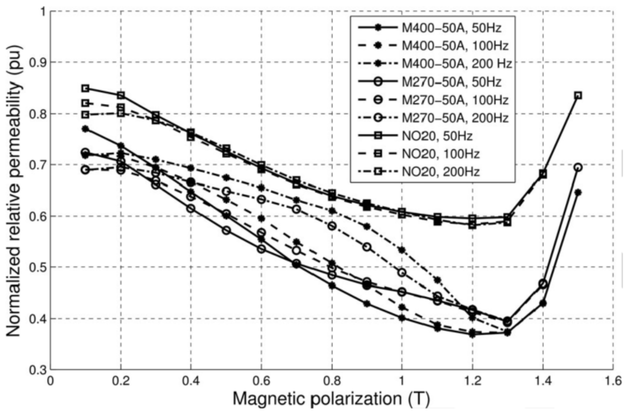


Fig.9 Normalized total specific loss of 10 mmm M400-50A strips at 50Hz, after cutting with guillotine shear and laser, with 30mm mechanically cut strips as reference.

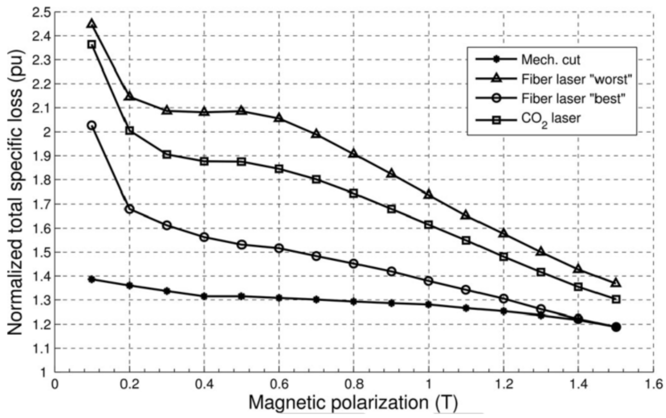


Fig. 10 Normalized relative permeability of 10 mm M400-50A strips at50 Hz, after cutting with guillotine shear and laser, with the 30 mm mechanically cut strips as reference

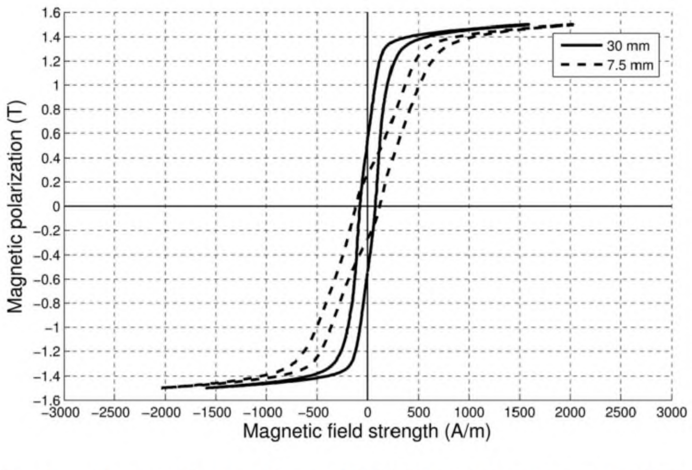


Fig. 11. Hysteresis loops of laser cut M270-50A with the best setting at 50 Hz for two different strip widths.

## V. WELDING EFFECT

Welding has also been investigated in the literature [23], [25]. However, in those references, measurements on ring core topology were conducted. In this study, a new method using Epstein measurements is proposed. The test specimens are standard Epstein strips (30 mm wide) of M400-50A laminations with one, three, five, and ten welding seams as depicted in Fig. 12. As reference, a nonwelded strip is used. All the specimens have ten welding sockets, where the welding can be applied. The welding is performed by welding two strips together, so that there will be a two over two strips overlap in the corners, which is a practical deviation to the singular lamination layer overlap in the standard Epstein method, but needed for accommodating the welding experiment. The possibility of finding the relative degradation caused by welding is enabled, since the reference, the non-welded strip, is also stacked with double overlaps in the corners.

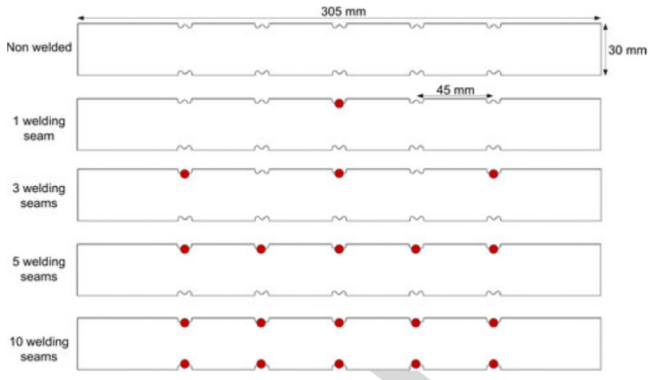


Fig. 12 Samples used for the investigation of the welding effect

The effective path length in the Epstein frame is 940 mm, according to the IEC 404-2 standard [1]. A method to investigate the effect of welding is the determination of the magnetic degradation as a function of the number of welding seams. The welding seams are equally distributed along the periphery of the Epstein frame.

Figs. 13 and 14 illustrate the trends of the total specific loss and the relative permeability as a function of the number of the welding seams. Welding at one side of the flux path introduces extra losses due to thermal residual stresses and local eddy currents. However, welding at both sides of the laminations also introduces extra eddy current losses in the total volume of strips between the welding seams. Table I summarizes the increase of the iron losses and the reduction of the relative permeability at an induction of 1 T and a frequency of 50 Hz.

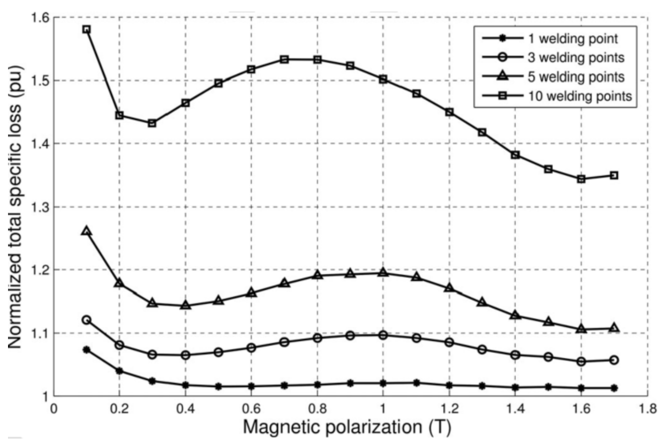


Fig 13. Normalized total specific loss of welded M400-50A laminations at 50 Hz, with non-welded laminations as reference.

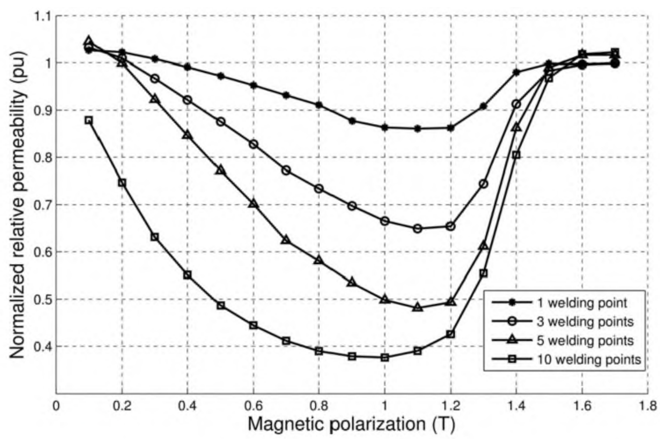


Fig. 14. Normalized relative permeability of welded M400-50A laminations at 50 Hz, with nonwelded laminations as reference.

TABLE I
DEVIATION OF IRON LOSS PER MASS UNIT AND RELATIVE PERMEABILITY DUE TO WELDING AT 1 T AND 50 HZ, WITH NONWELDED LAMINATIONS AS REFERENCE

| | 1 weld. seam | 3 weld. seams | 5 weld. seams | 10 weld. seams |
|---|---|---|---|---|
| Deviation of $p_{\mathrm{Fe}}$ | +2% | +10% | +19% | +50% |
| Deviation of $\mu_r$ | –14% | –34% | –50% | –62% |

It is found that the magnetic material is deteriorated as more welding seams are introduced. An increased total specific loss up to 50% at 1 T and a corresponding relative permeability drop of 62% are measured for the case with ten welding seams. However, this extreme case has double-sided welding seams, not commonly used in electrical machine manufacturing. This results in additional eddy-current losses due to the extra paths for circulating currents enclosing the path of the main magnetic flux, as well as extra residual thermal stresses introduced compared to the sample welded on one side. Even with only one welding seam per strip with a width of 30 mm, the steel is clearly degraded, especially for the relative permeability. Motors with a welded stator core periphery and a yoke thickness around 30 mm or less should therefore be expected to have significantly worse magnetic properties than before the welding process.

## VI. INCORPORATION OF CUTTING EFFECTS IN ELECTRICAL MACHINE MODELS

An original method to incorporate the cutting effect into a FEM model is proposed. It considers a homogenously damaged area as wide as the flux path defined by the sheet geometry in the same way as in [12], [14], [15], and [19]. However, the originality of the approach is that the geometry of the electrical machine is taken into consideration while choosing the B(H) curve and the iron loss coefficients valid for a specific part of the machine.

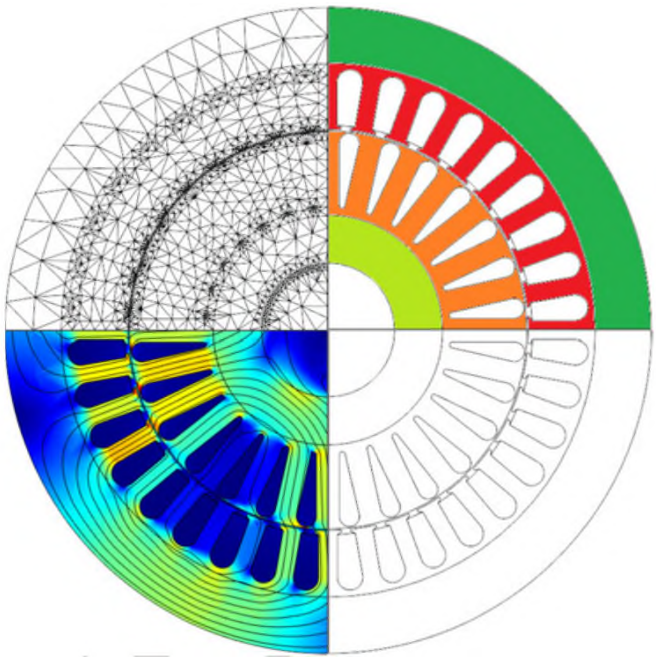

Fig. 15 Illustration of the FEM model of the induction motor which includes the modeled degradation profiles in the separated yoke and teeth regions.

In the model that is suggested in this paper, both stator and rotor are separated in teeth and yoke regions, as illustrated in Fig. 15. The properties of the magnetic material M270-50A that are assigned in each region, shown in the first quadrant, are based on Epstein measurements of strips with different widths. This means that the geometric dimensions of the motor, tooth widths for teeth regions and yoke widths for yoke regions, give the degradation profile to use. For instance, machines with higher numbers of slots give larger degradation, due to the resulting reduced widths of the teeth. In this study, the experimental results regarding the degradation of the electrical steel due to mechanical (guillotine) and laser cutting are implemented in the 2-D finite-element model of a low-voltage industrial induction motor.

The iron loss coefficients for hysteresis losses and eddy-current losses, respectively, are determined by surface fitting of the iron loss per mass unit versus frequency and induction based on the Epstein frame measurement results for 30-, 15-, 10-, and 7.5-mm-wide lamination strips, as illustrated in Fig. 16 for a strip width of 30 mm. The used fitting equation is the iron loss separation model with two terms, as given by

$$p_{\mathrm{Fe}} = p_{\mathrm{hyst}} + p_{\mathrm{ec}} = k_{\mathrm{hyst}} f \hat{B}^2 + k_{\mathrm{ec}} f^2 \hat{B}^2 \qquad (1)$$

where $p_{Fe}$ is the total iron loss per mass unit, $p_{hyst}$ is the hysteresis loss component, $p_{ec}$ is the eddy-current loss component, $k_{hyst}$ is the hysteresis loss coefficient, $k_{ec}$ is the eddy-current loss coefficient, f is the frequency, and B is the flux density [29].

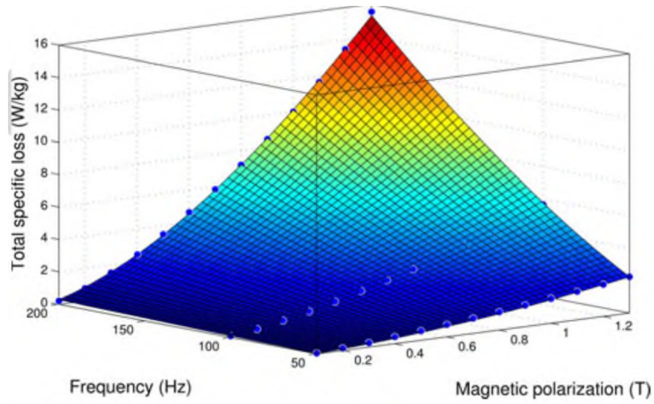


Fig. 16. Iron loss per mass unit versus frequency and flux density from measurements of M270-50A with markers for curve-fitting equation using determined loss coefficients.

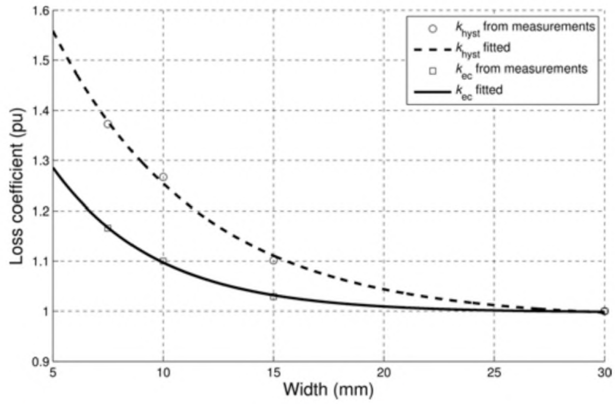


Fig. 17. Normalized hysteresis and eddy-current loss coefficients determined from measurements of M270-50A with different lamination strip widths and corresponding fitting curves for guillotine shearing.

The normalized iron loss coefficients for any lamination strip width are derived from the resulting fitting curves on the determined coefficients, as given in Fig. 17, for guillotine shearing of M270-50A. Similarly derived loss coefficients for other steel grades and manufacturing methods can be found in [26]. It is clearly seen in Fig. 17 that the hysteresis losses are more affected by degradation due to cutting than eddy-current losses, and is 27% and 10% higher, respectively, for a 10–mm-wide strip compared to the reference of 30 mm. Similar behavior was reported in [15]–[17]. The B(H) values for the FEM model are also based on measurement results, and linear interpolation is applied on the magnetic field strength for arbitrary widths in between tested strip widths for a given induction.

TABLE II
SIMULATION RESULTS OF A FOUR POLES INDUSTRIAL INDUCTION MOTOR WITH RATED POWER 7.5 KW AND M270-50A STEEL AT 50 HZ USING DEGRADATION PROFILES, WITH NO DEGRADATION PROFILE AS REFERENCE

| | **No degrad.** | **Mech. cutting** | **Laser *"best"*** | **Laser *"worst"*** |
|---|---|---|---|---|
| **Output power (p.u.)** | 0.5 | 0.5 | 0.5 | 0.5 |
| **Voltage (p.u.)** | 1 | 1 | 1 | 1 |
| **Current deviation (%)** | 0 | +3.7 | +2.2 | +6.2 |
| **Cosφ deviation (%)** | 0 | -3.2 | -1.7 | -4.9 |
| **Stator copper loss deviation (%)** | 0 | +7.5 | +4.4 | +12.8 |
| **Iron loss deviation (%)** | 0 | +15 | +31 | +51 |

The results of the time-stepping simulations for mechanically- and laser-cut core laminations are given in Table II, for a 7.5-kW-rated motor at 50% load. It is seen that the iron loss increase due to the material degradation varies between 15% and 50%, depending on the cutting technique. Additionally, the reduced permeability increases the stator current, resulting in a copper loss increase of roughly 4% to 13%, and the best laser gives the lowest deviation compared with no degradation as reference. The effects of the altered losses on a motor's performance are of course dependent on the motor design and the type of operation. Besides the obvious fact that the design of highly efficient motors becomes more complex, some general conclusions can be made to highlight certain areas of working points where the effects of the material degradation are pronounced. During high torque–low speed operation, a reduced permeability is of particular importance for the prediction of the copper losses and the winding temperature. Furthermore, at high speed operation, the increased iron losses can have a significant effect on the motor efficiency.

## VI. DISCUSSION

The main benefit of using Epstein tests is that this method is commonly used by steel manufacturers, and such data are in turn used as input for FEM models in machine design. Therefore, Epstein tests give unprecedented transparency on the manufacturing effects, especially when presented as in this paper by using normalized data. Ring cores, etc., give specific value, but the usefulness on other geometries and other sizes than what has been tested, is more uncertain, and is therefore estimated to be of a poorer value, if the main target is to create a general model.

Bali and Muetze [30] present a comparative table of different materials and effects of manufacturing based on different measurement methods. Putting this table together requires a huge effort since the community is presenting in general absolute values of losses. Even though the presented results are compared to a selected number of references, extensive comparison is outside the scope of this study since the first plausible explanation for the large variations is the mechanical properties of the magnetic material and its variation with parameters like chemical composition and grain size. The grain size is hardly ever reported, [10], [12], and [18] being exceptions, though it has been known for many years now that it is a major factor for the magnetic properties [31] and level of manufacturing degradation [18].

Combining the results presented in [20]–[22] with the local flux density measurements presented in [7] (assuming these are valid for other material grades), it seems advantageous to use a FE approach with a fixed thin damaged area for mechanical cutting modeling, while a continuous degradation is better suited to account for laser cutting effect. When there is a requirement to model both cutting techniques in a unified approach with minimal changes to existing FEM models, the uniformly damaged assumption combined with interpolation of measured properties accounting for flux path width presented in [26] and [27] may be good enough for industrial purposes.

Bali and Muetze [30] presents an extensive review of different ways to take into account manufacturing effects in electromagnetic device models. A good way to follow up the intensive activities in the research community on the subject is most probably to track new articles citing [30]. However, progress in the accuracy of predicted performance seldom goes in hand with easiness of implementation of the proposed methods and costs to acquire the input material data from an industrial perspective.

The material data implemented in the proposed model assume that each subarea has two cut edges. The effect of cutting on the stator yoke is well represented for normally more than 75% of it since the slot bottom has a cut edge. Typically less than 25% of the yoke only has one cut edge and the curvature of the geometry is not considered, though it has been shown it has an influence [13]. Further theoretical and experimental investigations are required to answer whether this has a major influence on the results. Taking into account the effect of rotational flux in this same area is most probably to be prioritized in order to improve the local iron loss predictions [15], [28].

## VIII. CONCLUSION

The relative degradations on total specific loss and relative permeability are investigated for the manufacturing methods guillotine shearing, laser cutting and welding, using the Epstein frame method. It is found that all manufacturing methods can have severe effects, if the dimension between the affected edges is small, and clear effects are evident at dimensions below 30 mm.

Mechanical cutting results in more than 20% iron loss increase and more than 40% relative permeability reduction at 1 T for M270-50A, for a strip width of 10 mm compared with the reference of 30 mm. The tested steel grade with thinner gauge show lower degradation. Moreover, steel grades with lower Si content show lower degradation at low induction, but at higher induction than 0.6 T the relative difference is small. It is also observed that the effect of frequency on the normalized degradation is insignificant, in the tested interval of 50–200 Hz.

Laser cut material has generally worse properties than mechanically cut counterparts except at high polarizations, where the relative permeability of laser cut material can be higher, where a crossing point at 1.3 T is identified. A fiber laser is furthermore found to outperform a $CO_2$ laser, regarding less material degradation. As fast and powerful settings as possible with the equipment are recommended, since these settings correspond to the least degradation of the magnetic properties and correspond as well to a faster manufacturing process, saving costs.

Welding experiments show an iron loss increase of more than 20% with a corresponding 50% reduction in the permeability compared to similar nonwelded M400-50A laminations.

A FEM model which includes a degradation profile is developed, where the magnetization and loss characteristics of the motor change according to the geometry. FEM simulations of an industrial induction motor rated 7.5 kW using M270-50A have indicated increase of up to 51% in the iron losses and up to 13% in the copper losses at partial load. These relative large performance deteriorations justify the implementation of the effect of cutting in industrial finite-element design tools using a method, which is based on material data relatively easy to obtain from electrical steel manufacturers and does not increase the FEM simulation times.

## REFERENCES


[1] *Methods of Measurement of the Magnetic Properties of the Electrical Steel Sheet and Strip by Means of Epstein Frame*, International Standard IEC404-2.
[2] T. Tanzer, H. Pregartner, A. Muetze, and K. Krischan, "Experimental determination of specific power losses and magnetostriction of electrical steel coils," in *Proc. IEEE Int. Conf. Elect. Mach.*, Lausanne, Switzerland, Sep. 2016, pp. 2230–2236.
[3] K. H. Schmidt, "Influence of punching on the magnetic properties of electric steel with 1% silicon," *J. Magn. Magn. Mater.*, vol. 2, pp. 136–150, Dec. 1975.
[4] A. Boglietti, "A first approach for the iron losses building factor determination," in *Proc. 34th IAS Annu. Meeting IEEE Ind. Appl. Conf.*, 1999, vol. 1, pp. 489–493.
[5] A. Moses, N. Derebasi, G. Loisos, and A. Schoppa, "Aspects of the cut-edge effect stress on the power loss and flux density distribution in electrical steel sheets," *J. Magn. Magn. Mater.*, vol. 215/216, pp. 690–692, Jun. 2000.
[6] A. Schoppa, J. Schneider, and J.-O. Roth, "Influence of the cutting process on the magnetic properties of non-oriented electrical steels," *J. Magn. Magn. Mater.*, vol. 215/216, pp. 100–102, Jun. 2000.
[7] R. Siebert, J. Schneider, and E. Beyer, "Laser cutting and mechanical cutting of electrical steels and its effect on the magnetic properties," *IEEE Trans. Magn.*, vol. 50, no. 4, Apr. 2014, Art. no. 2001904.
[8] M. Emura, F. Landgraf, W. Ross, and J. Barreta, "The influence of cutting technique on the magnetic properties of electrical steels," *J. Magn. Magn. Mater.*, vol. 254/255, pp. 358–360, 2003.
[9] P. Baudouin, A. Belhadj, F. Breaban, A. Deffontaine, and Y. Houbaert, "Effects of laser and mechanical cutting modes on the magnetic properties of low and medium Si content nonoriented electrical steels," *IEEE Trans. Magn.*, vol. 38, no. 5, pp. 3213–3215, Sep. 2002.
[10] A. Belhadj, P. Baudouin, F. Breaban, A. Deffontaine, M. Dewulf, and Y. Houbaert, "Effect of laser cutting on microstructure and on magnetic properties of grain non oriented electrical steels," *J. Magn. Magn. Mater.*,vol. 256, pp. 20–31, 2003.
[11] G. von Pfingsten, S. Steentjes, A. Thul, T. Herold, and K. Hameyer, "Soft magnetic material degradation due to manufacturing process: A comparison of measurements and numerical simulations," in *Proc. IEEE Int. Conf. Elect. Mach. Syst.*, Hangzhou, China, 2014, pp. 2018–2024.
[12] M. Hofmann, H. Naumoski, U. Herr, and H.-G. Herzog, "Magnetic properties of electrical steel sheets in respect of cutting: Micromagnetic analysis and macromagnetic modeling," *IEEE Trans. Magn.*, vol. 52, no. 2, Feb. 2016, Art. no. 2000114.
[13] M. Bali and A. Muetze, "Influences of $CO_2$ laser, FKL laser, and mechanical cutting on the magnetic properties of electrical steel sheets," *IEEE Trans. Ind. Appl.*, vol. 51, no. 6, pp. 4446–4454, Nov./Dec. 2015.
[14] I. J. Garshelis, G. Crevecoeur, S. P. L. Tollens, and L. Dupre, "Application of the drag force method to evaluate magnetic property degradation near the cut edges of electrical steels," *J. Appl. Phys.*, vol. 109, 2011, Art. no. 07E518.
[15] L. Vandenbossche, S. Jacobs, X. Jannot, M. McClelland, J. Saint-Michel, and E. Attrazic, "Iron loss modelling which includes the impact of punching, applied to high efficiency induction machines," in *Proc. 3rd Int. Elect. Drives Prod. Conf.*, 2013, pp. 1–10.
[16] W. M. Arshad *et al.*, "Incorporating lamination processing and component manufacturing in electrical machine design tools," in *Proc. 42nd Annu. Meeting IEEE Ind. Appl. Soc.*, New Orleans, LA, USA, Sep. 2007, pp. 94–102.
[17] W. M. Arshad, T. Ryckebusch, A. Broddefalk, F. Magnussen, H. Lendenmann, and M. Lindenmo, "Characterization of electrical steel grades for direct application to electrical machine design tools," *J. Magn. Magn. Mater.*, vol. 320, no. 20, pp. 2538–2541, Oct. 2008.
[18] S. K. Kuo, W. C. Lee, S. Y. Lin, and C. Y. Lu, "The influence of cutting edge deformations on magnetic performance degradation of electrical steel," *IEEE Trans. Ind. Appl.*, vol. 51, no. 6, pp. 4357–4363, Nov./Dec. 2015.
[19] Z. Gmyrek, A. Cavagnino, and L. Ferraris, "Estimation of the magnetic properties of the damaged area resulting from the punching process: Experimental research and FEM modeling," *IEEE Trans. Ind. Appl.*, vol. 49, no. 5, pp. 2069–2077, Sep./Oct. 2013.
[20] T. P. Holopainen, P. Rasilo, and A. Arkkio, "Identification of magnetic properties for cutting edge of electrical steel sheets," in *Proc. IEEE Int. Conf. Elect. Mach.*, Lausanne, Switzerland, Sep. 2016, pp. 1783–1787.
[21] P. Rasilo, U. Aydin, T. P. Holopainen, and A. Arkkio, "Analysis of iron losses on the cutting edges of induction motor core laminations," in *Proc. IEEE Int. Conf. Elect. Mach*, Lausanne, Switzerland, Sep. 2016, pp. 1312–1317.
[22] S. Elfgen, S. Steentjes, S. B¨ ohmer, D. Franck, and K. Hameyer, "Influences of material degradation due to laser cutting on the operating behaviour of PMSM using a continuous local material model," in *Proc. IEEE Int. Conf. Elect. Mach.*, Lausanne, Switzerland, Sep. 2016, pp. 1835–1840.
[23] A. Schoppa, J. Schneider, C.-D. Wuppermann, and T. Bakon, "Influence of welding and sticking of laminations on the magnetic properties of non-oriented electrical steels," *J. Magn. Magn. Mater.*, vol. 254/255, pp. 367–369, 2003.

[24] A. Boglietti, A. Cavagnino, L. Ferraris, and M. Lazzari, "The annealing influence onto the magnetic and energetic properties in soft magnetic material after punching process" in *Proc. IEEE Elect. Mach. Drives Conf.*, Jun. 2003, vol. 1, pp. 503–508.
[25] A. Krings, S. Nategh, O. Wallmark, and J. Soulard, "Influence of the welding process on the magnetic properties of a slot-less permanent magnet synchronous machine stator core," in *Proc. IEEE Int. Conf. Elect. Mach.*, Marseille, France, Sep. 2012, pp. 1333–1338.
[26] K. Bourchas, "Manufacturing effects on iron losses in electrical machines," M.Sc. thesis, Royal Inst. Technol., Stockholm, Sweden, 2015.
[27] K. Bourchas *et al.*, "Influence of cutting and welding on magnetic properties of electrical steels," in *Proc. IEEE Int. Conf. Elect. Mach.*, Lausanne, Switzerland, Sep. 2016, pp. 1815–1821.
[28] Y. Liu, S. K. Kashif, and A. M. Sohail, "Engineering considerations on additional iron losses due to rotational fields and sheet cutting," in *Proc. 18th IEEE Int. Conf. Elect. Mach.*, Vilamoura, Portugal, Sep. 2008, pp. 1–4.
[29] H. Jordan, "Die ferromagnetischen konstanten fur schwache wechselfelder," *Elektr. Nach. Techn.*, vol. 1, p. 8, 1924.
[30] M. Bali and A. Muetze, "Modeling the effect of cutting on the magnetic properties of electrical steel sheets," *IEEE Trans. Ind. Electron.*, vol. 64, no. 3, pp. 2547–2556, Mar. 2017.
[31] E. T. Stephenson and A. R. Marder, "The effects of grain size on the core loss and permeability of motor lamination steel," *IEEE Trans. Magn.*, vol. MAG-22, no. 2, pp. 101–106, Mar. 1986.

**Konstantinos Bourchas** was born in Athens, Greece, in 1989. He received the diploma degree in electrical and computer engineering from the National Technical University of Athens, Athens, Greece, in 2012, and the M.Sc. degree in electric power engineering from the KTH Royal Institute of Technology, Stockholm, Sweden, in 2015.
In 2015, he elaborated his master thesis in ABB LV Motors, Västerås, Sweden. He is currently a Motor Design Engineer in the automotive industry. His research interests include magnetic materials and losses in electrical machines, and design and modeling of electrical machines.

**Alexander Stening** was born in 1979, in Stockholm, Sweden. He received the M.Sc., Licentiate, and Ph.D. degrees in electrical engineering from the Royal Institute of Technology (KTH), Stockholm, Sweden, in 2006, 2010, and 2013, respectively. In 2013 he joined ABB LV Motors, Sweden, as a Development Engineer. He is currently with ABB Traction Motors, Sweden, as a Senior Development Engineer. His current research interests include electrical machines and drives.

**Juliette Soulard** (M'00) received the Ph.D. degree in Electrical Engineering from the University of Paris VI, France, in 1998. She was Associate Professor with the Department of Electric Power and Energy Systems, leading the Electrical Machines and Drives laboratory at KTH Royal Institute of Technology, Stockholm, Sweden at the time this study was conducted. Since September 2016, she is associate professor at the International Automotive Research Center, within WMG, University of Warwick, United Kingdom, focusing on advanced propulsion system applications. Her research interests include modelling and design of electrical machines, especially losses, manufacturing effects and thermal modelling.

**Arvid Broddefalk** received the M.Sc degree in materials physics from Uppsala University, Sweden, in 1995 and the Ph.D. degree in magnetic materials in 2000 at the same university. Since 2001 he has been working at Cogent Surahammars Bruk on the development of the magnetic properties of electrical steel, especially on low loss grades and thin grades for high frequency applications.

**Magnus Lindenmo** had in 1982 a M.Sc. in metallurgy from Royal Institute of Technology in Stockholm, Sweden. He has worked with Swedish Institute for Metals Research (now KIMAB) in Stockholm and with ABB Powdermet. Since 1993 he has worked on electrical steels with Cogent Surahammars Bruk on quality, development and customer technical support and is currently managing the two latter functions.

**Mats Dahlén** has a B.Sc. in Business Administration and Economics from Blekinge Institute of Technology. He started as a production engineer at ABB Nordkomponent in 2006 and has been active in the field of sheet metal processing for more than a decade. He is currently the Manager of Production Engineering and Development at AQ Components Västerås, Sweden.

**Freddy Gyllensten** (M'01) received the M.Sc. degree in electrical engineering from Chalmers University of Technology, Gothenburg, Sweden, in 1994 and the Ph.D. degree in electrical machines and drives from the Royal Institute of Technology (KTH), Stockholm, Sweden, in 2004. Since 1996 until 2010, he has been with ABB Corporate Research, Sweden, as Scientist and Project Manager in various development projects. Since 2010 through 2014, he has been with ABB LV Motors, Sweden, as R&D Manager. He is currently with ABB Motors and Generators, Sweden, as Senior Principal Engineer. His research interests include electrical machines and drives. He is the author or coauthor of more than thirty papers and is the inventor or co-inventor of a dozen patents. He is a member of IEEE and a member of IEC, in the national committee of Sweden and in international working groups within electrical machines standardization.